Computers in Biology and Medicine 155 (2023) 106695

Contents lists available at ScienceDirect

Computers in Biology and Medicine

journal homepage: www.elsevier.com/locate/compbiomed

# Differentiating between stress- and EPT-induced electrodermal activity during dental examination

Youngsun Kong [a,*], Hugo F. Posada-Quintero [a], Hanh Tran [b], Ankur Talati [b], Thomas J. Acquista [a], I-Ping Chen [b], Ki H. Chon [a]

[a] Biomedical Engineering, University of Connecticut, Storrs, CT, 06269, USA
[b] Department of Oral Health and Diagnostic Sciences, University of Connecticut Health, Farmington, CT, 06032, USA

ARTICLE INFO

*Keywords:*
Electrodermal activity
Pain
Stress
Electrical pulp test
Endodontic diagnosis
Pulpal diagnosis
Machine learning

ABSTRACT

Dental pain invokes the sympathetic nervous system, which can be measured by electrodermal activity (EDA). In the dental clinic, accurate quantification of pain is needed because it could enable optimized drug-dose treatments, thereby potentially reducing drug addiction. However, a confounding factor is that during pain there is also lingering residual stress, hence, both contribute to the EDA response. Therefore, we investigated whether EDA can differentiate stress from pain during dental examination. The use of electrical pulp test (EPT) is an ideal approach to tease out the dynamics of stress and mimic pain with lingering residual stress. Once the electrical sensation is felt and reaches a critical current threshold, the subject removes the probe from their tooth, hence, this stage of data represents largely EPT stimulus and the residual stress-induced EDA response is smaller. EPT was performed on necrotic and vital teeth in fifty-one subjects. We defined four different data groups of reactions based on each individual's EPT intensity level expectation based on the visual analog scale (VAS) of their baseline trial, as follows: mild stress, mild stress + EPT, strong stress, and strong stress + EPT. EDA-derived features exhibited significant difference between residual lingering stress + EPT groups and stress groups. We obtained 84.6% accuracy with 76.2% sensitivity and 86.8% specificity with multilayer perceptron in differentiating between pure-stress groups vs. stress + EPT groups. Moreover, EPT induced much greater EDA amplitude and faster response than stress. Our finding suggests that our machine learning approach can discriminate between stress and EPT stimulation in EDA signals.

## 1. Introduction

Dental treatments are time-sensitive so prompt diagnosis is of the utmost importance. However, dental stress can cause some patients to avoid timely diagnosis and dental care [1,2]. This is further emotionally ingrained as dental stress can lead to avoidance of dental visits, which can exacerbate dental problems, leading to more stressful dental treatments [3,4]. Hence, unduly high stress can delay timely treatment when it can be most effective. A prior work has shown that the pain experienced during treatment is significantly correlated with stress [5,6]. However, pain is currently assessed using subjective scales [4,5,7], which can be affected by biological, sociocultural, and psychological factors [8–10]. These can hamper accurate dental assessment for children, the deaf, and others with communication issues. Thus, quantifying pain can lead to more effective treatment, and provide positive feedback to subjects and less stress towards the treatments, which can further lead to more acceptance of preventive and timely dental care.

Recently, electrodermal activity (EDA) was shown to be a sensitive surrogate physiological marker for sympathetic arousal (e.g., pain, cognitive stress, and emotion) [11]. EDA measures the changes in electrical conductance of the skin modulated by the opening of the sweat glands, which are controlled by the sympathetic nervous system. Consequently, researchers have explored the use of EDA to detect and quantify various sympathetic stimuli with good results [12–17]. In our previous research, we have used features derived from EDA based on time signals and time-frequency analysis, as well as EDA's differential features, for the assessment of pain elicited by heat and electrical stimuli. In this prior study we showed statistically significant differences for multi- and binary-levels of heat and electrical pain, and accurate pain assessment using machine-learning classifiers [12–15]. Other research groups have also successfully detected heat pain using EDA signals with deep learning approaches [16,17].

* Corresponding author. 407 Engineering and Science Building, 67 N Eagleville Rd, Storrs, University of Connecticut Storrs, CT, 06269, USA.
*E-mail address:* youngsun.kong@uconn.edu (Y. Kong).

https://doi.org/10.1016/j.compbiomed.2023.106695
Received 27 October 2022; Received in revised form 20 December 2022; Accepted 14 February 2023
Available online 15 February 2023

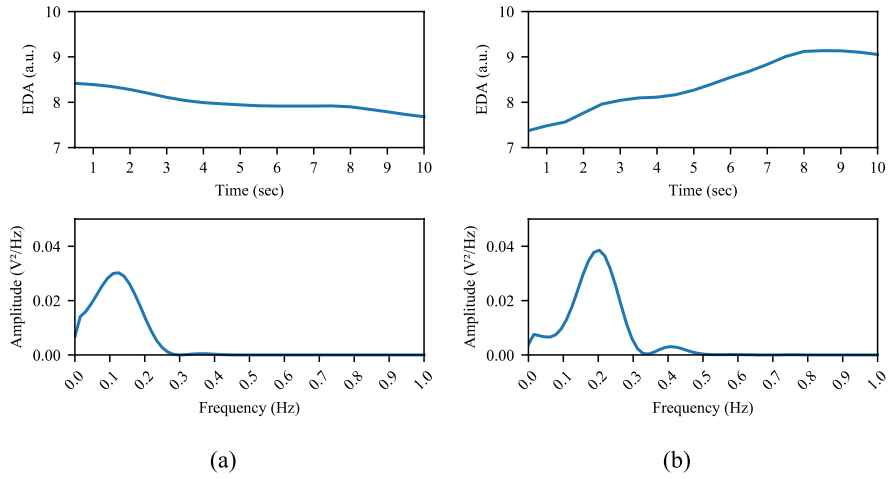


**Fig. 1.** Representative PSDs of EDA signals with (a) stress and (b) stress + EPT (EPT result of 49/80).

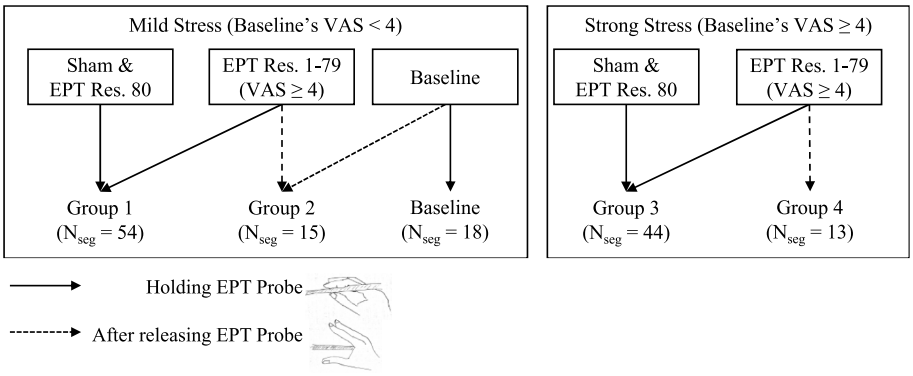


**Fig. 2.** Scheme of group segmentation. Baseline refers to the first EPT for each subject.

Stress which is sensed at the amygdala can also elicit responses in EDA via the sympathetic nervous system [18–22]. Most pain studies consider stress as a confounding factor. There have been no research studies that have tried to differentiate stress from other sympathetic stimuli in EDA signals. Sugimine et al. showed that normalized skin conductance level (nSCL) which was developed to differentiate different heat pain can discriminate heat, mechanical, and cold pain from stress (e.g., audio and visual stimuli) in EDA signals [23,24]. However, the fact that pain and stress were not elicited to a subject at the same time limits their study as both stimuli affect to each other and to EDA signals [25]. Moreover, the experiment was conducted in well-controlled environment including 5–10 min of waiting time with closing the eyes and 20 s of pre-stimulus time with opening the eyes. Thus, their study precludes the aim to separate pain dynamics from other sympathetic stimulus causing stress.

The aim of this work was to investigate whether or not we can differentiate between stress and pain perception during dental examination involving electrical pulp test (EPT). We chose EPT because placement of the EPT probe on a tooth induces stress without any sensation at first, followed by the actual electrical stimulus thereafter. The full effect of EPT stimulus is delayed because the current placed on the tooth is cumulative—after it reaches a certain threshold, the EPT sensation is felt. Hence, EPT sensation on a tooth is a delayed response. Thus, we hypothesize that EPT is a good model for measuring only stress, followed by the pain-mimicking sensation elicited by the electrical stimulus, albeit with some residual lingering stress [26].

## 2. Methods

### 2.1. Participants

All studies involving human protocols were in accordance with guidelines of the Institutional Review Board of the University of Connecticut Health (IRB protocol 20-043-1). We recruited patients who had one tooth that required a root canal treatment and two nearby normal teeth. We excluded patients under the age of 18, pregnant women, those with profound anxiety (Corah's dental anxiety scale ≥15, ranging 4–20) based on survey questions, having porcelain-crowned teeth, taking medications with anticholinergic side effects which can affect skin conductance, prior sympathectomy procedures, and those diagnosed with Raynaud's syndrome. Twenty-seven females and twenty-four males, for a total of fifty-one patients (aged 35.78 ± 11.81) were recruited, with Corah's anxiety levels of 7.04 ± 2.59.

### 2.2. Stimuli and materials

#### 2.2.1. Electric pulp test (EPT)

The electric pulp test (EPT) was used to test EDA using a Vitality Scanner 2006 (Kerr Dental, Orange, CA, USA). A conductance gel, toothpaste, was applied to the tip of the EPT probe. Patients were asked to hold the EPT probe to complete the circuit and start delivery of current to a tooth and to release the EPT probe as soon as they felt sensation on the tooth. Mainkar and Kim reported in 2018 that sensitivity and specificity of testing non-vital and vital teeth using EPT are estimated to be 72% and 93%, respectively from their meta-analysis of 28 studies in

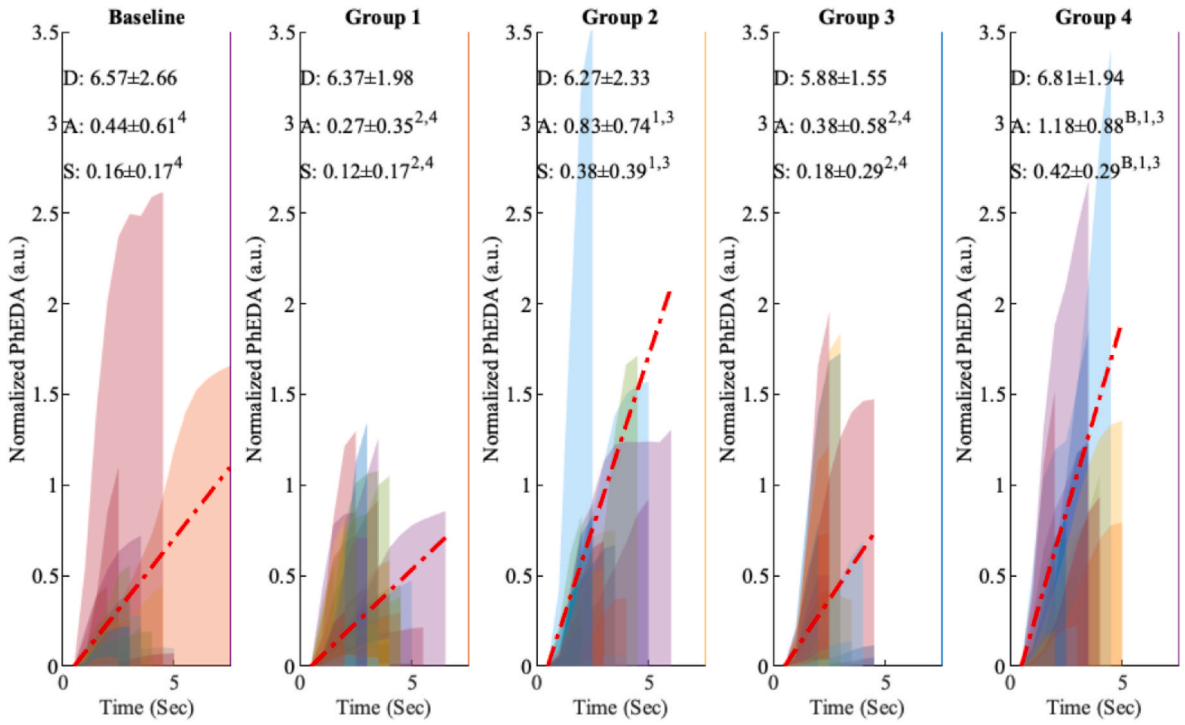


**Fig. 3.** Comparison of normalized PhEDA. Varying colors denote different segments. Red dashed lines indicate averaged slopes. 'D', 'A', and 'S' represent duration, amplitude, and slope, respectively. Superscript indices indicate which groups show significant difference with that level ($p < 0.05$).

2018 [27]. Therefore, EPT is one of the standard clinical tests performed for pulp diagnosis.

### 2.2.2. Electrodermal activity (EDA)

EDA signals can be decomposed into two salient components, phasic (i.e., rapid change) and tonic (i.e., slow change) components [11]. The phasic component, defined as the skin conductance response (SCR), accounts for a rapid increase in EDA amplitude in response to activation of the sympathetic response to a stimulus [11,28]. The tonic component of EDA, known as skin conductance level (SCL), is a slower response than SCR [11]. As we aim to differentiate pain-mimicking stimuli from stress in EDA signals, we selected only the phasic component of EDA, as both stress and (especially) pain responses have faster dynamics than SCL. We also calculated time-frequency spectral analysis features as they have been shown to provide more sensitivity to the sympathetic activity (e.g., pain) than the phasic and tonic components of EDA [13,19,29]. Moreover, we computed the differential characteristic features derived from the phasic component of EDA, as they has been shown to be a good discriminant [13].

EDA was collected using a clinical-grade galvanic skin response device (GSR AMP, ADInstrument, Sydney, Australia) and an amplifier (PowerLab, ADInstrument, Sydney, Australia) from the index and middle fingers, using reusable stainless-steel electrodes. The EDA signals were collected at 1000 Hz using the LabChart 8 software (ADInstrument, Sydney, Australia). The collected data were resampled to 8 Hz, then passed through a median filter with 16 samples corresponding to 2 s, to remove motion artifacts in the EDA signals. The filtered signals were then resampled to 2 Hz for further processing of EDA features, including the power spectral density (PSD) of EDA signals [19], the phasic component of EDA (decomposed using cvxEDA and the derivative of the phasic signals (dPhEDA) [13]), the time-varying index of sympathetic activity (TVSymp), and modified TVSymp (MTVSymp) [13,29].

*2.2.2.1. Power spectral density (PSD) of EDA signals.* We hypothesize that pain perception induced by EPT has faster dynamics compared to stress. To investigate this, the power spectral density (PSD) was used to find the dominant frequency and its amplitude for both stress + EPT and stress only signals. We computed PSD using the Welch function in the SciPy library [30] for the filtered EDA, after detrending. The PSD of the EDA signal is the measure of power in the EDA signal with a function of frequency [31]. The PSD is a good analysis tool to compare if EDA signals between stress and stress + EPT have different amplitude and response speed. For example, a subject obtained 0.125 Hz with amplitude 0.030 $V^2$/Hz and 0.203 Hz with 0.039 $V^2$/Hz for before and after the EPT on a vital tooth, respectively (EPT result 49/80, Fig. 1).

*2.2.2.2. Phasic component of EDA (PhEDA) and derivative of phasic signals (dPhEDA).* We used cvxEDA to decompose phasic and tonic components of EDA signals and to extract phasic driver [32]. We also calculated the derivative of the phasic signals (dPhEDA) as this accentuates fast changes [13]. To calculate dPhEDA, we applied the five-point stencil central finite differences equation [33] as follows:

$$dphEDA_n = \frac{p_{n-2} - 8 \bullet p_{n-1} + 8 \bullet p_{n+1} - p_{n+2}}{12 \bullet (1/F_s)} \quad \text{(Eq. 1)}$$

where p and $F_s$ represent a phasic component of EDA extracted using cvxEDA and the sampling frequency of 2 Hz, respectively.

*2.2.2.3. Time-varying index of sympathetic activity (TVSymp) and modified TVSymp.* We also calculated TVSymp and MTVSymp, which have been shown to provide some of the highest sensitivities to sympathetic arousals including both pain and stress [13]. First, we applied a highpass filter at 0.01 Hz. The key part of TVSymp computation is to use a variable frequency complex demodulation (VFCDM) approach next to extract frequency components in the 0.08–0.24 Hz range. VFCDM has been shown to exhibit one of the highest time and frequency spectral resolutions while maintaining accurate amplitude estimates. The third step of TVSymp computation is to estimate instantaneous amplitudes from the decomposed components so that a reconstruction of the signal of interest can be made. Following is a summary of the second and third steps of the TVSymp computational procedures from a previous

**Table 1**
Comparison of EDA with statistic features (Mean ± Standard deviation).

| EDA Feature | | Baseline | Group 1 | Group 2 | Group 3 | Group 4 |
|---|---|---|---|---|---|---|
| PSD | Dominant Freq. * | 0.11 ± 0.06 | 0.13 ± 0.12 | 0.13 ± 0.05 | 0.13 ± 0.13 | 0.12 ± 0.05 |
| | Amplitude | 0.55 ± 2.03 | 0.08 ± 0.19$^{2,4}$ | 1.34 ± 3.69$^{1,3}$ | 0.20 ± 0.70$^{2,4}$ | 1.26 ± 3.82$^{1,3}$ |
| PhEDA | Approx. Entropy | 0.01 ± 0.05$^{2}$ | 0.00 ± 0.01$^{2,4}$ | 0.02 ± 0.08 $^{B,1,3}$ | 0.01 ± 0.02$^{2}$ | 0.03 ± 0.08$^{1}$ |
| | Max | 2.80 ± 5.67 | 4.14 ± 16.19$^{2,4}$ | 7.30 ± 23.36$^{1,3}$ | 0.87 ± 1.26$^{2,4}$ | 2.77 ± 2.68$^{1,3}$ |
| | Mean | 2.24 ± 5.19 | 3.75 ± 15.87$^{2,4}$ | 6.52 ± 23.32$^{1,3}$ | 0.49 ± 0.81$^{2,4}$ | 1.92 ± 1.93$^{1,3}$ |
| | Min | 1.72 ± 4.53 | 3.38 ± 15.58$^{2}$ | 5.62 ± 23.13$^{1,3}$ | 0.27 ± 0.52$^{2,4}$ | 0.98 ± 1.40$^{3}$ |
| | S.D. | 0.33 ± 0.47 | 0.24 ± 0.57$^{2,4}$ | 0.53 ± 0.50$^{1,3}$ | 0.18 ± 0.25$^{2,4}$ | 0.57 ± 0.51$^{1,3}$ |
| dPhEDA | Approx. Entropy | 0.11 ± 0.11$^{2,3,4}$ | 0.07 ± 0.12$^{2,4}$ | 0.25 ± 0.13 $^{B,1,3}$ | 0.05 ± 0.10 $^{B,2,4}$ | 0.27 ± 0.13 $^{B,1,3}$ |
| | Max | 0.33 ± 0.55$^{2,4}$ | 0.16 ± 0.33$^{2,4}$ | 0.79 ± 1.00 $^{B,1,3}$ | 0.20 ± 0.40$^{2,4}$ | 0.85 ± 1.30 $^{B,1,3}$ |
| | Mean | 0.01 ± 0.19$^{4}$ | 0.01 ± 0.20$^{4}$ | 0.02 ± 0.18 | −0.03 ± 0.08$^{4}$ | 0.07 ± 0.16 $^{B,1,3}$ |
| | Min | −0.24 ± 0.35 | −0.12 ± 0.20$^{2}$ | −0.49 ± 0.69$^{1,3}$ | −0.17 ± 0.26$^{2}$ | −0.41 ± 0.64 |
| | S.D. | 0.17 ± 0.24$^{1}$ | 0.08 ± 0.10 $^{B,2,4}$ | 0.34 ± 0.45 $^{B,1,3}$ | 0.10 ± 0.16$^{2,4}$ | 0.33 ± 0.45$^{1,3}$ |
| Ph. Driver | Approx. Entropy | 0.08 ± 0.11$^{2,4}$ | 0.05 ± 0.11$^{2,4}$ | 0.20 ± 0.14 $^{B,1,3}$ | 0.06 ± 0.12$^{2,4}$ | 0.25 ± 0.21 $^{B,1,3}$ |
| | Max | 4.61 ± 8.81$^{3}$ | 5.02 ± 17.15$^{2,4}$ | 11.45 ± 30.01$^{1,3}$ | 1.40 ± 2.47 $^{B,2,4}$ | 6.91 ± 9.44$^{1,3}$ |
| | Mean | 1.71 ± 4.11$^{3}$ | 2.91 ± 12.46$^{2,4}$ | 5.10 ± 18.30$^{1,3}$ | 0.32 ± 0.55 $^{B,2,4}$ | 1.63 ± 1.56$^{1,3}$ |
| | Min | 0.01 ± 0.05 | 1.26 ± 8.51 | 1.47 ± 7.19 | 6.77e-05 ± 2.27e-04 | 1.15e-04 ± 4.64e-04 |
| | S.D. | 1.21 ± 2.14$^{3}$ | 1.22 ± 3.91$^{2,4}$ | 2.92 ± 7.20$^{1,3}$ | 0.38 ± 0.63 $^{B,2,4}$ | 1.82 ± 2.11$^{1,3}$ |
| TVSymp | Approx. Entropy | 0.01 ± 0.03$^{2}$ | 0.01 ± 0.03$^{2}$ | 0.05 ± 0.06 $^{B,1,3}$ | 0.00 ± 0.01$^{2}$ | 0.05 ± 0.07 |
| | Max | 1.71 ± 1.31$^{1,3}$ | 1.04 ± 1.00 $^{B,2,4}$ | 2.67 ± 1.30$^{1,3}$ | 1.02 ± 1.24 $^{B,2,4}$ | 2.82 ± 1.92$^{1,3}$ |
| | Mean | 1.04 ± 0.94$^{1,3}$ | 0.59 ± 0.65 $^{B,2,4}$ | 1.74 ± 0.91$^{1,3}$ | 0.49 ± 0.56 $^{B,2,4}$ | 1.83 ± 1.22$^{1,3}$ |
| | Min | 0.47 ± 0.62$^{1,3}$ | 0.24 ± 0.37 $^{B,2,4}$ | 0.62 ± 0.54$^{1,3}$ | 0.19 ± 0.23 $^{B,2,4}$ | 0.87 ± 0.68$^{1,3}$ |
| | S.D. | 0.39 ± 0.34 | 0.24 ± 0.24$^{2,4}$ | 0.70 ± 0.35$^{1,3}$ | 0.25 ± 0.35$^{2,4}$ | 0.62 ± 0.47$^{1,3}$ |
| MTVSymp | Approx. Entropy | 0.04 ± 0.08$^{2}$ | 0.02 ± 0.05$^{2,4}$ | 0.09 ± 0.10 $^{B,1,3}$ | 0.01 ± 0.04$^{2,4}$ | 0.10 ± 0.10$^{1,3}$ |
| | Max | 0.53 ± 0.51 | 0.31 ± 0.41$^{2,4}$ | 0.95 ± 0.60$^{1,3}$ | 0.34 ± 0.53$^{2,4}$ | 1.03 ± 0.85$^{1,3}$ |
| | Mean | 0.15 ± 0.18 | 0.09 ± 0.14$^{2,4}$ | 0.31 ± 0.25$^{1,3}$ | 0.08 ± 0.14$^{2,4}$ | 0.34 ± 0.30$^{1,3}$ |
| | Min | 0 ± 0 | 0 ± 0 | 0 ± 0 | 0 ± 0 | 0 ± 0 |
| | S.D. | 0.18 ± 0.18 | 0.10 ± 0.14$^{2,4}$ | 0.36 ± 0.25$^{1,3}$ | 0.11 ± 0.17$^{2,4}$ | 0.37 ± 0.32$^{1,3}$ |

Superscript indices indicate which levels show significant difference with that level ($p < 0.05$).

publication [29]. We define $x(t)$ to be a narrow band oscillation with a center frequency $f_0$, instantaneous $A(t)$, phase $\varphi(t)$, and the direct current component $dc(t)$, as follows:

$$x(t) = dc(t) + A(t)\cos(2\pi f_0 t + \varphi(t)). \quad \text{Eq. (2)}$$

By multiplying Eq. (2) by $e^{-j2\pi f_0 t}$, the instantaneous amplitude information $A(t)$ and phase information $\varphi(t)$ can be extracted for a given center frequency, resulting in:

$$z(t) = dc(t)e^{-j2\pi f_0 t} + \frac{A(t)}{2}e^{j\varphi(t)} + \frac{A(t)}{2}e^{-j(4\pi f_0 t + \varphi(t))}. \quad \text{Eq. (3)}$$

The center frequency $f_0$ then can move to zero frequency in the spectrum of $z(t)$ by shifting $e^{-j2\pi f_0 t}$ to the left. With an ideal low-pass filter (LPF) $z(t)$ with a cutoff frequency $f_c < f_0$, the filtered signal $z_{lp}(t)$ will contain only the component of interest as follows:

$$z_{lp}(t) = \frac{A(t)}{2}e^{j\varphi(t)} \quad (4)$$

$$A(t) = 2\left|z_{lp}(t)\right| \quad (5)$$

$$\varphi(t) = arctan\left(\frac{\text{imag}\left(z_{lp}(t)\right)}{\text{real}\left(z_{lp}(t)\right)}\right). \quad (6)$$

If the modulating frequency varies as a function of time, the signal x (t) can be expressed as follows:

$$x(t) = dc(t) + A(t)\left(\int_0^t \cos(2\pi f(\tau)d\tau + \varphi(t))\right) \quad (7)$$

Similar to Eqs. (2) and (3), both instantaneous amplitude, A(t), and instantaneous phase $\varphi(t)$ can be produced by multiplying Eq. (7) by $e^{-j\int_0^t 2\pi f(\tau)d\tau}$ as follows:

$$z(t) = x(t)e^{-j\int_0^t 2\pi f(\tau)d\tau} = dc(t)e^{-j\int_0^t 2\pi f(\tau)d\tau} + \frac{A(t)}{2}e^{j\varphi(t)} + \frac{A(t)}{2}e^{-j\int_0^t 4\pi f(\tau)d\tau} \quad (8a)$$

From Eq. (8), the filtered signal $z_{lp}(t)$ can be obtained with the same instantaneous amplitude A(t) and phase φ(t) as provided in Eqs. (5) and (6) by applying an ideal LPF to z(t) with a cutoff frequency $f_c < f_0$. The instantaneous frequency can be obtained as follows:

$$f(t) = f_0 + \frac{1}{2\pi}\frac{d\varphi(t)}{dt} \quad (8b)$$

The 2 Hz EDA signal was used to obtain TVSymp in the previous publication [29], where VFCDM decomposed the signals with 2 Hz sampling frequency with the centered spectral frequencies consisting of 0.04, 0.12, 0.20, 0.28, 0.36, 0.44, 0.52, 0.60, 0.68, 0.76, 0.84, and 0.92 Hz. The second and third components were added to include the sympathetic dynamics ranging between 0.045 and 0.25 Hz. The reconstructed signal was normalized to unit variance. Instantaneous amplitudes of the summed value can be obtained using the Hilbert transform as follows:

$$Y'(t) = \frac{1}{\pi}p.v\int_{-\infty}^{\infty}\frac{X'(\tau)}{t-\tau}d\tau \quad (9)$$

where p.v represents the Cauchy principal value. An analytic signal, Z (t), can be defined with the complex conjugate pair $X^*$ (t) and $Y^*$(t), as follows:

$$\begin{aligned} Z(t) = X'(t) + iY'(t) = a(t)e^{j\theta(t)}\ a(t) = \left[X'2(t) + Y'2(t)\right]^{1/2}\ \theta(t) \\ = \arctan(Y'(t)\,/\,X'(t)) \end{aligned} \quad (10)$$

TVSymp a(t) is obtained with the instantaneous amplitude of Z(t). Finally, we calculated MTVSymp from TVSymp to emphasize EDA signals driven by sympathetic arousal and remove other baseline EDA responses from the prior segments. MTVSymp has shown higher sensitivity to detect pain in our previous publications [13,34]. MTVSymp was calculated as follows:

$$MTVSymp_t = \begin{cases} a_t - \mu_t, \mu_t \le a_t \\ 0, \mu_t > a_t \end{cases}, \mu_t = \frac{1}{k \bullet F_s}\sum_{i=t-5\bullet F_{rs}}^{t-1} a_i \quad (11)$$

where $F_s$ represents the sampling frequency of 2 Hz.

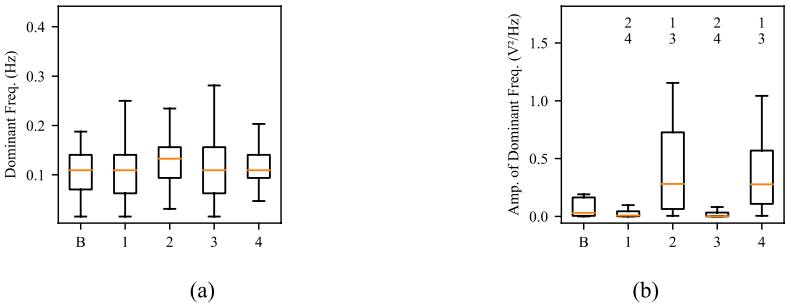


**Fig. 4.** (a) Dominant frequency and (b) its PSD. Labels for the x-axes represent 1) Baseline (mild stress), 2) mild stress 3) EPT sensation/mild stress 4) strong stress and 5) EPT sensation/strong stress. The numbers represent other groups from which that group is significantly different. Outliers were omitted, which were set if each datum is above Q1 − 1.5 × (Q3 − Q1) or below Q3 + 1.5 × (Q3 − Q1). Q1 and Q3 represent the first and third quartiles, respectively.

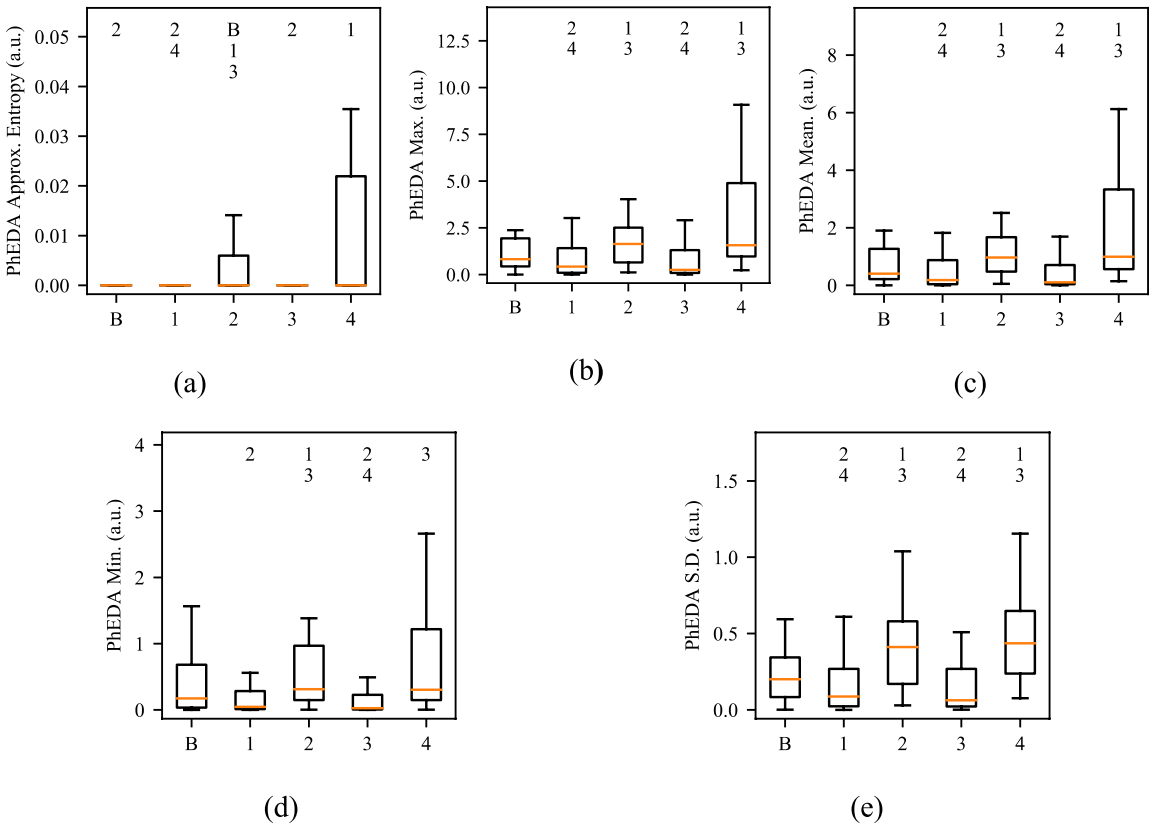


**Fig. 5.** Boxplots of PhEDA. Labels for the x-axes represent 1) Baseline (mild stress), 2) mild stress 3) EPT sensation/mild stress 4) strong stress and 5) EPT sensation/strong stress. The numbers and 'B' represent other groups from which that group is significantly different. Outliers were omitted, which were set if each datum is above Q1 − 1.5 × (Q3 − Q1) or below Q3 + 1.5 × (Q3 − Q1). Q1 and Q3 represent the first and third quartiles, respectively.

### 2.3. Design and procedure

Patients were examined in endodontic clinic at UConn Health. While patients were in a dental chair in the supine position, EDA electrodes were placed on the index and middle fingers. Patients were briefed about the EPT test procedure and encouraged to ask any questions they had. Patients were told to relax for 2-min baseline measurements, followed by EPT tests on a vital tooth and a necrotic tooth. The EPT scale (0–80) at the point when the patient released the probe was recorded for each test. After each EPT test, patients were asked to report their visual analogue scale (VAS) score on a scale from 0 to 10. A sham test was used on a vital tooth as there were twenty subjects without a necrotic tooth. Note that EPT on a necrotic tooth ideally causes only pure stress, as does the sham test.

EPT delivers current while a probe was placed on a tooth and held by a patient. When current reaches a threshold of electrical sensation (i.e., EPT result 1–79/80) or the maximum value (i.e., EPT result 80/80) for the vital tooth and non-vital tooth, respectively. EPT causes pure stress regardless of a tooth condition, followed by an electrical stimulus with some residual stress for vital teeth. We segmented the data into four different categories with a baseline (Fig. 2). The baseline involves EPT data that were collected for each subject before an EPT stimulus was applied. As indicated earlier, most subjects have mild stress based on a survey of their anxiety levels (Corah's anxiety levels of 7.04 ± 2.59). Hence, we considered this group to have mild stress. For each subject, the first EPT level highly influences the stress levels for the rest of the

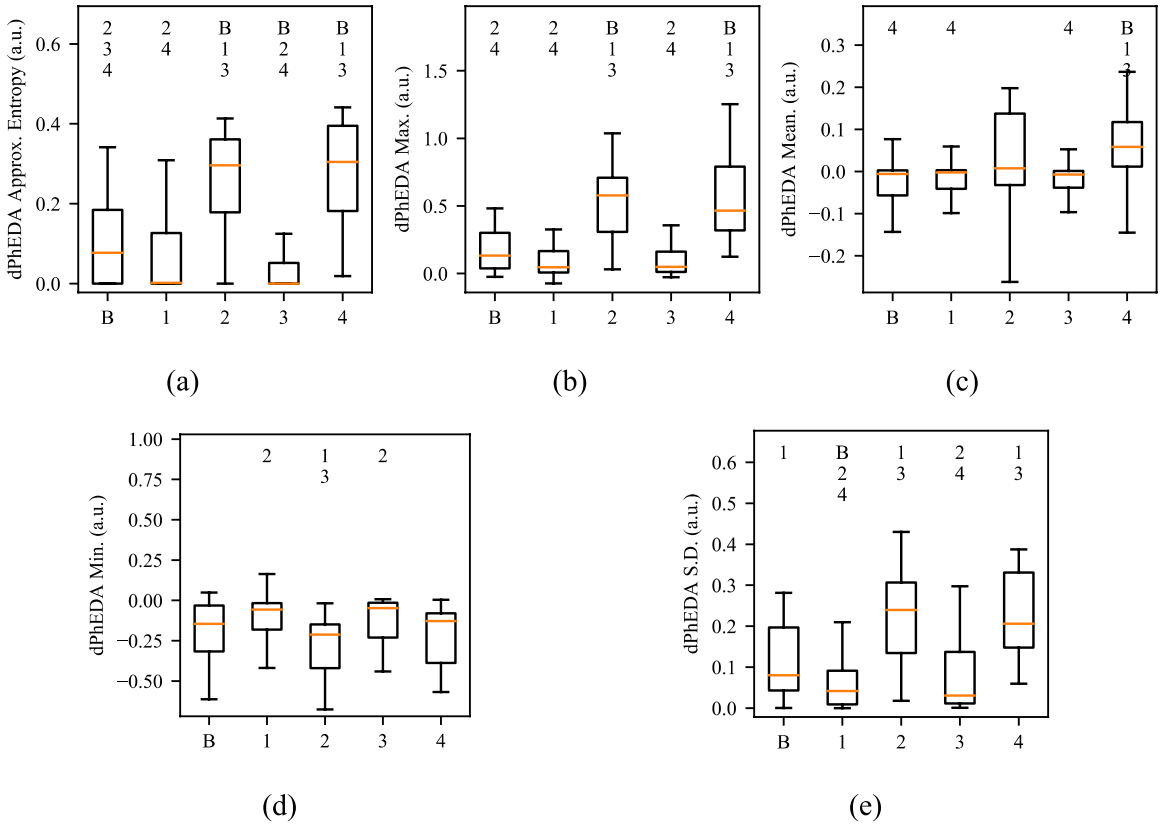


**Fig. 6.** Boxplots of dPhEDA. Labels for the x-axes represent 1) Baseline (mild stress), 2) mild stress 3) EPT sensation/mild stress 4) strong stress and 5) EPT sensation/strong stress. The numbers and 'B' represent other groups from which that group is significantly different. Outliers were omitted, which were set if each datum is above Q1 − 1.5 × (Q3 − Q1) or below Q3 + 1.5 × (Q3 − Q1). Q1 and Q3 represent the first and third quartiles, respectively.

segments to be either mild or strong. We considered patients to have strong stress if the VAS obtained from the first EPT (elicited only on vital teeth) was 4 or greater (groups 3 and 4), while they are considered to have mild stress if VAS was less than 4 (groups 1 and 2). If the EPT induced a sensation (neither sham test nor necrotic tooth), we set EPT stimulus with mild stress to be group 2 and with strong stress + EPT to be group 4. Before the EPT induced a sensation, we set mild stress to be the baseline for the first EPT trial, and group 1 for the rest of trials, and strong stress to be the group 3. We took 10-s segments of EDA data for each group categorization. To summarize, baseline, groups 1 and 3 correspond to when the EPT probe was on a tooth, while groups 2 and 4 represent after the EPT probe was released (Fig. 2). Note that we consider that some degree of stress was always present during the experiments.

### 2.4. Statistics and machine learning

We calculated five statistical measures for each EDA feature (phEDA, dphEDA, phasic driver of EDA, TVSymp, MTVSymp) consisting of the approximate entropy, maximum, mean, minimum, and standard deviation. The minimum of MTVSymp was discarded due to all zero values. Approximate entropy's parameters of $m$ and $r$ are generally recommended to be 2 and 0.2 times the standard deviation of the signal [35,36]. Thus, the parameters $m$ and $r$ were set to 2 and 0.2 multiplied by standard deviation of EDA data from a previously-collected dataset consisting of 10 subjects (five females and five males) undergoing pain (heat) and stress (the Stroop test) [37]. Kruskal-Wallis H test was used to compare EPT and stress segments, followed by Dunn's test with Bonferroni correction, as they were non-normally distributed. We used the Kolmogorov-Smirnov test to determine the normality of each group. A p-value $<0.05$ was considered statistically significant.

We also examined machine learning algorithms to classify EPT stimuli from pure stress segments. The machine learning approaches consisted of support vector machine (SVM) with a linear kernel, logistic regression (LR), random forest (RF), and multi-layer perceptron (MLP), using Python 3.9 with the Sckit-learn library 0.24.2. We used leave-one-subject-out cross-validation to minimize the overfitting and procure subject independence of our results. For each fold, the following steps were conducted. First, SVM-Synthetic-Minority-Oversampling-Technique (SMOTE) was performed to make training datasets balanced [38]. Standardization was then done with zero mean and unit variance, except for random forest. Features were selected using the same classifiers based on feature importance greater than the average value of feature importance, except for MLP for which features were selected using Perceptron. Hyper parameters of the machine-learning algorithms were selected using grid-search-cross-validation with group five-fold cross-validation based on geometric mean score, as follows:

$$Geometric\ mean\ score = \sqrt{sensitivity \bullet specificity} \tag{12}$$

Parameter C for both SVM and LR was chosen from 0.01, 0.1, 1, 10, 100, and 1000. For RF, four different depths (3, 4, 5, and 6) were tested to calculate feature importance with the Gini criterion. Finally, MLP was tested with three different number of hidden layers (1, 2, and 3), with 100 hidden units, rectifier linear unit activation function, the Adam optimizer, and 0.001 learning rate.

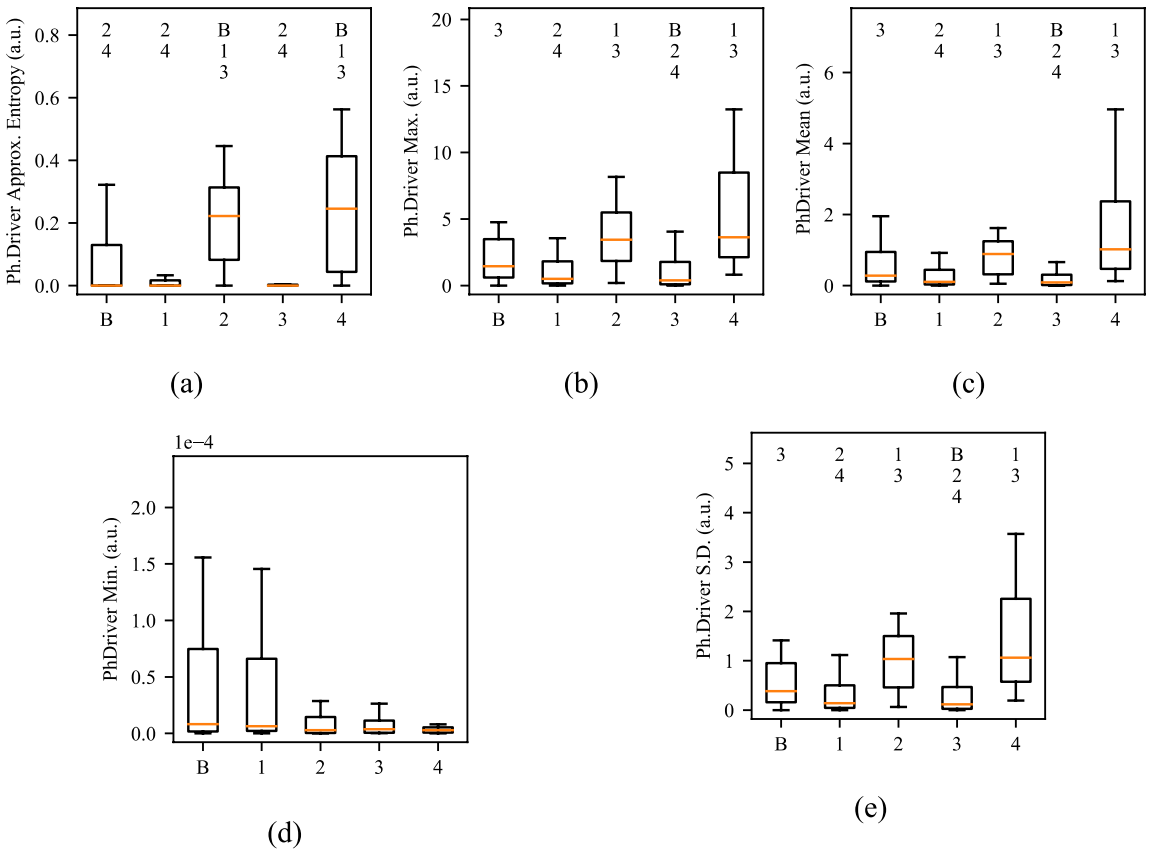


**Fig. 7.** Boxplots of Phasic Driver. Labels for the x-axes represent 1) Baseline (mild stress), 2) mild stress 3) EPT sensation/mild stress 4) strong stress and 5) EPT sensation/strong stress. The numbers and 'B' represent other groups from which that group is significantly different. Outliers were omitted, which were set if each datum is above Q1 − 1.5 × (Q3 − Q1) or below Q3 + 1.5 × (Q3 − Q1). Q1 and Q3 represent the first and third quartiles, respectively.

## 3. Results

### 3.1. Normalized phasic component of EDA

To compare between background stress and sensation elicited by EPT, we calculated normalized PhEDA signals during onset-to-peak time for all segments, adjusted to have zero amplitude at onset (Fig. 3). Duration of PhEDA responses for each group was similar among all groups, while their amplitudes and slopes showed significant differences between stress + EPT (groups 2 and 4) and stress groups (groups 1 and 3). EPT with strong stress (group 4) exhibited a higher averaged slope than that with mild stress (group 2). Likewise, strong stress (group 3) showed a slightly higher average of amplitudes and slopes than mild stress (group 1). Baseline's averaged amplitude was higher than stress groups (groups 1 and 3), likely because more anxiety was experienced by the subjects during the first trial.

### 3.2. EDA features

All EDA's approximate entropy, max, mean, standard deviation features showed significant difference between stress and stress + EPT except for PSD (Table 1). Dominant frequency of PSD did not show significant difference between stress (groups 1 and 3) and stress + EPT groups (groups 2 and 4). Its stress groups had higher standard deviation than its stress + EPT groups. On the other hand, we observed a significant difference between EPT (groups 2 and 4) and stress groups (groups 1 and 3) for the amplitude of dominant frequency (Fig. 4).

All statistical features of the phasic component of EDA (PhEDA) exhibited significant differences between EPT (groups 2 and 4) and stress groups (groups 1 and 3), except for the approximate entropy values between strong stress and EPT + strong stress, and the minimum values between mild stress and EPT + strong stress (Fig. 5). Group with EPT + strong stress (group 4) was distributed within greater values than were group with EPT + mild stress (group 2), although there their median values were similar.

Approximate entropy, maximum, and standard deviation of dPhEDA showed significant differences between EPT (groups 2 and 4) and stress groups (groups 1 and 3), with higher median values of EPT groups (Fig. 6). Mean and minimum values of dPhEDA in EPT + mild stress group (group 2) were significantly different with groups 1 and 3, respectively. All statistical features of baseline's dPhEDA except for minimum exhibited significant difference with at least one of the other groups.

Except for the minimum values of the phasic driver of EDA, significant differences were observed between EPT (groups 2 and 4) and stress groups (groups 1 and 3, Fig. 7). Also, maximum, mean, and standard deviation of baseline's phasic drivers of EDA showed a significant difference with the strong stress group (group 3). Approximate entropy of baseline's phasic driver showed significant difference with EPT groups (groups 2 and 4). Except for the minimum value and approximate entropy of the phasic driver of EDA, EPT with strong stress (group 4) were distributed within greater values than were EPT with mild stress (group 2), although their median values were similar (Fig. 7).

TVSymp showed significant differences between EPT (groups 2 and 4) and stress groups (groups 1 and 3, Fig. 8), except for approximate entropy. All statistical features of baseline's TVSymp showed significant difference with at least one of the other groups, except for standard deviation. Approximate entropy showed significant difference between

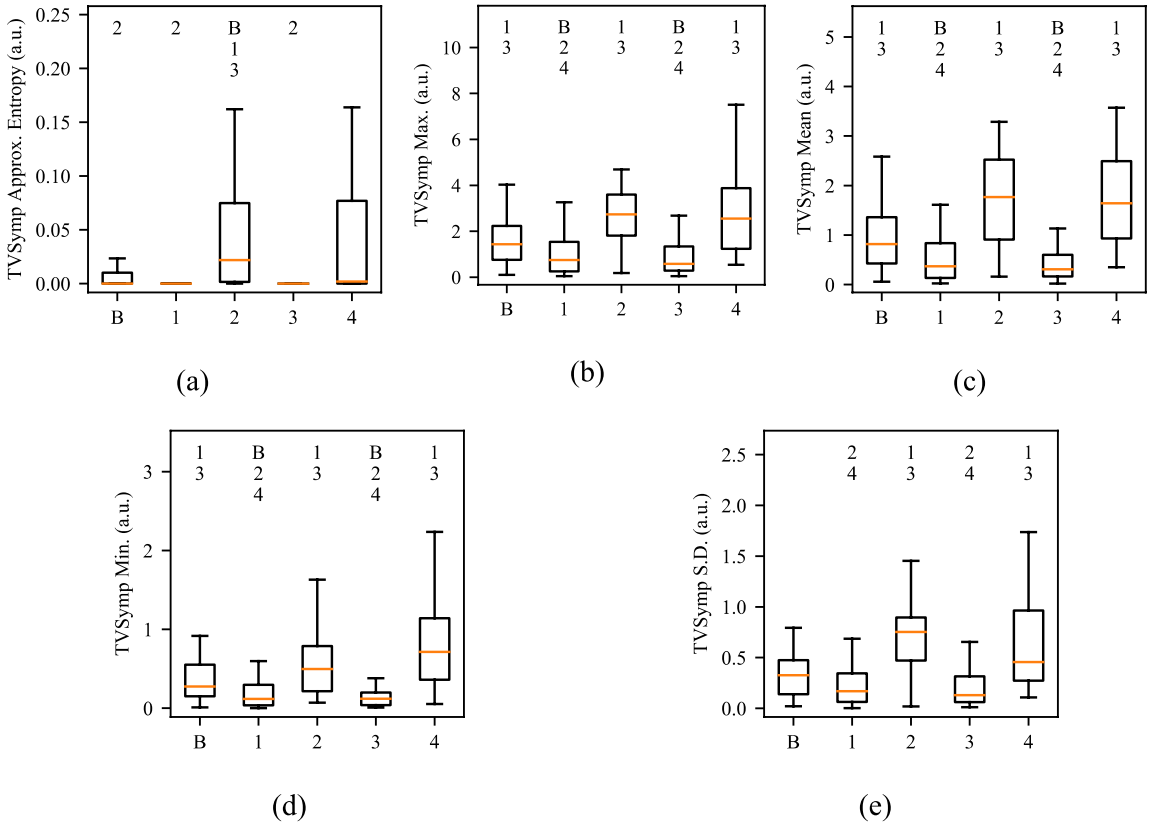


**Fig. 8.** Boxplots of TVSymp. Labels for the x-axes represent 1) Baseline (mild stress), 2) mild stress 3) EPT sensation/mild stress 4) strong stress and 5) EPT sensation/strong stress. The numbers and 'B' represent other groups from which that group is significantly different. Outliers were omitted, which were set if each datum is above Q1 − 1.5 × (Q3 − Q1) or below Q3 + 1.5 × (Q3 − Q1). Q1 and Q3 represent the first and third quartiles, respectively.

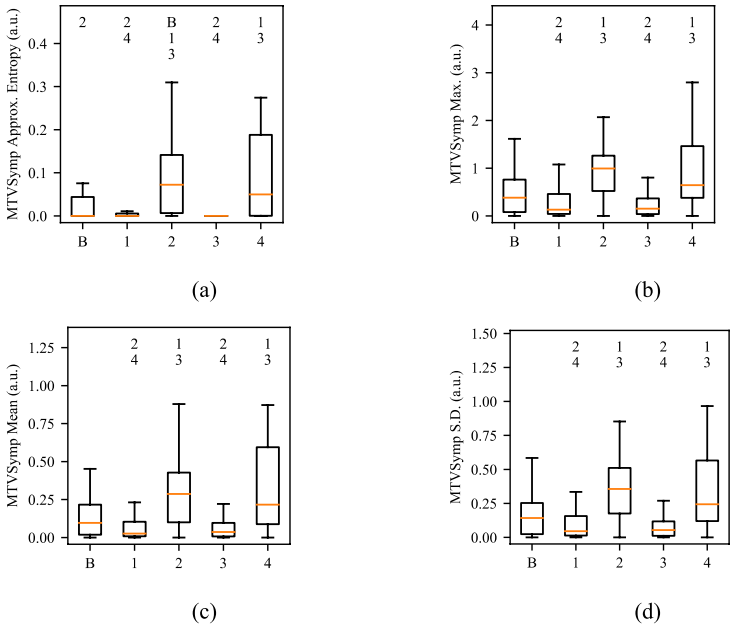


**Fig. 9.** Boxplots of MTVSymp. Labels for the x-axes represent 1) Baseline (mild stress), 2) mild stress 3) EPT sensation/mild stress 4) strong stress and 5) EPT sensation/strong stress. The numbers and 'B' represent other groups from which that group is significantly different. Outliers were omitted, which were set if each datum is above Q1 − 1.5 × (Q3 − Q1) or below Q3 + 1.5 × (Q3 − Q1). Q1 and Q3 represent the first and third quartiles, respectively.

**Table 2**
Classification results (EPT + stress vs. pure stress).

| | Baseline + Groups 1-4 | | | | Groups 1-4 | | | |
|---|---|---|---|---|---|---|---|---|
| | Acc. (%) | Sen. (%) | Spe. (%) | G1 (%) | Acc. (%) | Sen. (%) | Spe. (%) | G1 (%) |
| ***LR*** | 78.8 | 64.3 | 82.0 | 72.6 | *82.1* | *66.7* | *86.2* | *75.8* |
| ***SVML*** | 77.5 | 69.0 | 79.4 | 74.0 | *76.6* | *66.7* | *79.2* | *72.7* |
| RF | 80.5 | 52.4 | 86.6 | 67.4 | 83.6 | 64.3 | 88.7 | 75.5 |
| MLP | 81.8 | 64.3 | 85.6 | 74.2 | 84.6 | 76.2 | 86.8 | 81.3 |

| Baseline + Groups 1–4 (MLP, G1 = 74.2%) | | | | Groups 1–4 (MLP G1 = 81.3%) | | | | |
|---|---|---|---|---|---|---|---|---|
| | | Predicted Stress | | | | | Predicted Stress | |
| | | | Stress + EPT | | | | | Stress + EPT |
| True | Stress | 85.6% (166) | 14.4% (28) | | True | Stress | 86.7% (138) | 13.3% (21) |
| | Stress + EPT | 35.7% (15) | 64.3% (27) | | | Stress + EPT | 23.8% (10) | 76.2% (32) |

EPT with mild stress (group 2) and stress and baseline groups. MTVSymp also showed significant differences between EPT and stress groups (Fig. 9). The minimum of MTVSymp was excluded in our analysis as it is expected to be zero for all groups.

### 3.3. Machine learning

We obtained more than 76% of accuracy of the four classifiers with target EPT (groups 2 and 4) vs. stress (groups 1 and 3), as shown in Table 2. MLP obtained the highest accuracy and geometric mean score of 84.6% and 81.3%, respectively, with sensitivity of 76.2% and specificity of 86.8%. Random forest obtained a higher specificity than the other classifiers, with 88.7%, but lower sensitivities with 64.3%, respectively. With including baseline into stress group, our overall accuracy was slightly lower.

## 4. Discussion

We examined if EDA signals consisting of stress only and lingering stress + EPT can be accurately classified using features derived from EDA via machine learning. Our results showed that stress only and lingering stress + EPT can be distinguished using EDA features. All EDA features presented in the paper showed significant difference between stress (groups 1 and 3) and lingering stress + EPT groups (groups 2 and 4). Although no significant difference was observed between low and high stress groups, all of our features showed values that were distributed in a higher number range for the strong stress + EPT group than for the mild stress + EPT group. Interestingly, all EDA features for the baseline group (i.e., mild stress with the first trial for each subject) exhibited higher amplitude than other stress groups, and those differences were significant in several cases. This suggests that it could be possible to reduce outliers by inducing some trials before dental procedures when using EDA signals for pain or stress quantification. This is potentially due to learning effect as patients become more comfortable and less stressed due to familiarity with the experiments. With the selected features derived from EDA from various techniques, we obtained up to 84.6% accuracy with 76.2% sensitivity and 86.8% specificity with machine-learning techniques.

Previously, we have shown that features developed in our lab (e.g., dPhEDA, TVSymp, and MTVSymp) are highly sensitive to sympathetic stimuli elicited by cognitive stress, heat and electrical pain. Our new findings show that these features are also feasible for distinguishing lingering stress + EPT from stress only. Moreover, other traditional features such as phasic EDA and phasic driver of EDA also showed significant difference between EPT and lingering stress + EPT. The features developed in our lab all showed similarly consistent difference between mild stress and higher stress, while the traditional features (e.g., phasic EDA and phasic driver of EDA) showed inconsistent results. This suggests that features developed in our lab provide more consistent and accurate results in differentiating between those with stress versus stress and pain.

It has been shown that both sensation and anticipation of pain involve the same brain regions (e.g., anterior cingulate cortex, thalamus, and insular cortex) [39,40]. Both pain sensation and stress responses activate sympathetic outflows, which cause changes in skin blood flow and skin conductance responses [39]. Hence, given that both stress and pain sensation involve the same brain region, it is difficult to differentiate them. However, our results show that sympathetic skin response was stronger and exhibited faster dynamics during pain sensations induced by EPT (i.e., EPT + stress) than during the anticipation stage which, as noted, was prior to EPT inducing sufficient current to induce pain sensation (i.e., stress only). This type of behavior was also shown in a study in which heat pain induced in the volar forearm significantly increased EDA response, more so than did its anticipation [39]. Hence, EPT is a good model to induce both stress and pain sensation, as the beginning stage of EPT does not induce a noxious stimulus due to a delay in reaching the threshold current. Instead, stress is induced by anticipation followed by pain sensation when the required threshold of the current is reached with EPT. Our findings with EPT suggest that pulpal diagnosis using EDA can be accurately made whether stress is presented.

Despite our promising results, there are some limitations that need to be addressed in future studies. First, we did not consider low VAS (VAS <4), to minimize confounding factors in the study, as it might be ambiguous to define low VAS to be either EPT or other types of discomfort caused by purely anxiety and/or stress sensation. Also, we only recruited patients whose Corah's anxiety scale was less than 15, to exclude patients who could possibly experience other emotions than stress, such as fear. In future studies, more emotions, such as fear, should be considered. Moreover, EDA signals may vary depending on gender, sex, ethnicity, race, genetic background, and type of EDA device [37,41–43]. These factors should be considered in future studies. Another concern is that we evoked electrical sensation and stress using EPT but not actual dental pain, which may cause different effects and perceived pain. Further variations involving actual dental pain must be studied in the future.

## 5. Conclusions

We compared EDA features between stress and lingering stress + EPT. Our EDA features showed significant difference between stress and lingering stress + EPT segments. We found that the main differentiating observation between EPT and stress is that the former induced greater amplitude and faster response in EDA than the latter. Machine learning algorithms trained with a set of statistical features obtained from our EDA signal processing tools were able to discriminate lingering stress + EPT from only stress events with high accuracy, sensitivity and specificity. Our finding provides an approach based on EPT to discriminate between stress and pain with some degree of confidence. Hence, EPT is a good procedure to discriminate between pain and stress sensation via EDA.

## Declaration of competing interest

None.

## Acknowledgements

This research was funded by National Institute of Health (NIH/NIDCR) DE029563 to IP.C. and K.C.

## References

[1] A.M. White, L. Giblin, L.D. Boyd, The prevalence of dental anxiety in dental practice settings, Am Dental Hygien. Assoc. 91 (2017) 30–34.
[2] B.O. Gaffar, A.S. Alagl, A.A. Al-Ansari, The prevalence, causes, and relativity of dental anxiety in adult patients to irregular dental visits, Saudi Med. J. 35 (2014) 598–603.
[3] A.J. Van Wijk, J. Hoogstraten, Anxiety and pain during dental injections, J. Dent. 37 (2009) 700–704.
[4] S. Sanikop, P. Agrawal, S. Patil, Relationship between dental anxiety and pain perception during scaling, J. Oral Sci. 53 (2011) 341–348.
[5] S.K. Mp, Relationship between dental anxiety and pain experience during dental extractions, Asian J. Pharmaceut. Clin. Res. (2017) 458–461.
[6] K. Okawa, T. Ichinohe, Y. Kaneko, Anxiety may enhance pain during dental treatment, Bull. Tokyo Dent. Coll. 46 (2005) 51–58.
[7] B. Wondimu, G. Dahllof, Attitudes of Swedish dentists to pain and pain management during dental treatment of children and adolescents, Eur. J. Paediatr. Dent. 6 (2005) 66.
[8] L.C. Callister, Cultural influences on pain perceptions and behaviors, Home Health Care Manag. Pract. 15 (2003) 207–211.
[9] I. Kvachadze, M.G. Tsagareli, Z. Dumbadze, An Overview of Ethnic and Gender Differences in Pain Sensation, Georgian Medical News, 2015, pp. 102–108.
[10] K.M. Woodrow, G.D. Friedman, A.B. Siegelaub, M.F. Collen, Pain tolerance: differences according to age, sex and race, Psychosom. Med. 34 (1972) 548–556.
[11] H.F. Posada-Quintero, K.H. Chon, Innovations in electrodermal activity data collection and signal processing: a systematic review, Sensors 20 (2020) 479.
[12] H.F. Posada-Quintero, Y. Kong, K. Nguyen, C. Tran, L. Beardslee, L. Chen, T. Guo, X. Cong, B. Feng, K.H. Chon, Using electrodermal activity to validate multilevel pain stimulation in healthy volunteers evoked by thermal grills, Am. J. Physiol. Regul. Integr. Comp. Physiol. 319 (2020) R366. –R375.
[13] Y. Kong, H. Posada-Quintero, K. Chon, Sensitive Physiological Indices of Pain Based on Differential Characteristics of Electrodermal Activity, IEEE Transactions on Bio-Medical Engineering, 2021.
[14] Y. Kong, H.F. Posada-Quintero, K.H. Chon, Real-time high-level acute pain detection using a smartphone and a wrist-worn electrodermal activity sensor, Sensors 21 (2021) 3956.
[15] H.F. Posada-Quintero, Y. Kong, K.H. Chon, Objective pain stimulation intensity and pain sensation assessment using machine learning classification and regression based on electrodermal activity, Am. J. Physiol. Regul. Integr. Comp. Physiol. 321 (2) (2021) R186–R196.
[16] S.A.H. Aqajari, R. Cao, E.K. Naeini, M.-D. Calderon, K. Zheng, N. Dutt, P. Liljeberg, S. Salanterä, A.M. Nelson, A.M. Rahmani, Pain assessment tool with electrodermal activity for postoperative patients: method validation study, JMIR MHealth and UHealth 9 (2021), e25258.
[17] D. Lopez-Martinez, R. Picard, Continuous pain intensity estimation from autonomic signals with recurrent neural networks, 2018, in: 40th Annual International Conference of the IEEE Engineering in Medicine and Biology Society (EMBC), IEEE, 2018, pp. 5624–5627.
[18] M. Svetlak, P. Bob, M. Cernik, M. Kukleta, Electrodermal complexity during the Stroop colour word test, Auton. Neurosci. 152 (2010) 101–107.
[19] H.F. Posada-Quintero, J.P. Florian, A.D. Orjuela-Cañón, T. Aljama-Corrales, S. Charleston-Villalobos, K.H. Chon, Power spectral density analysis of electrodermal activity for sympathetic function assessment, Ann. Biomed. Eng. 44 (2016) 3124–3135.
[20] H.F. Posada-Quintero, J.P. Florian, A.D. Orjuela-Cañón, K.H. Chon, Electrodermal activity is sensitive to cognitive stress under water, Front. Physiol. 8 (2018) 1128.
[21] H. Feng, H.M. Golshan, M.H. Mahoor, A wavelet-based approach to emotion classification using EDA signals, Expert Syst. Appl. 112 (2018) 77–86.
[22] J. Shukla, M. Barreda-Angeles, J. Oliver, G.C. Nandi, D. Puig, Feature extraction and selection for emotion recognition from electrodermal activity, IEEE Trans. Affect. Comput. 12 (2019) 857–869.
[23] S. Sugimine, S. Saito, T. Takazawa, Normalized skin conductance level could differentiate physical pain stimuli from other sympathetic stimuli, Sci. Rep. 10 (2020) 1–12.
[24] R. Treister, M. Kliger, G. Zuckerman, I.G. Aryeh, E. Eisenberg, Differentiating between heat pain intensities: the combined effect of multiple autonomic parameters, PAIN® 153 (2012) 1807–1814.
[25] A.H. Ahmad, R. Zakaria, Pain in times of stress, Malays. J. Med. Sci.: MJMS 22 (2015) 52.
[26] J.C. Willer, Anticipation of pain-produced stress: electrophysiological study in man, Physiol. Behav. 25 (1980) 49–51.
[27] A. Mainkar, S.G. Kim, Diagnostic accuracy of 5 dental pulp tests: a systematic review and meta-analysis, J. Endod. 44 (2018) 694–702.
[28] G. Bohlin, Delayed habituation of the electrodermal orienting response as a function of increased level of arousal, Psychophysiology 13 (1976) 345–351.
[29] H.F. Posada-Quintero, J.P. Florian, Á.D. Orjuela-Cañón, K.H. Chon, Highly sensitive index of sympathetic activity based on time-frequency spectral analysis of electrodermal activity, Am. J. Physiol. Regul. Integr. Comp. Physiol. 311 (2016), https://doi.org/10.1152/ajpregu.00180.2016. R582–R591.
[30] P. Virtanen, R. Gommers, T.E. Oliphant, M. Haberland, T. Reddy, D. Cournapeau, E. Burovski, P. Peterson, W. Weckesser, J. Bright, SciPy 1.0: fundamental algorithms for scientific computing in Python, Nat. Methods 17 (2020) 261–272.
[31] J. Dempster, Chapter SIX - signal analysis and measurement, in: J. Dempster (Ed.), The Laboratory Computer, Academic Press, London, 2001, pp. 136–171, https://doi.org/10.1016/B978-012209551-1/50039-8.
[32] A. Greco, G. Valenza, A. Lanata, E.P. Scilingo, L. Citi, cvxEDA, A convex optimization approach to electrodermal activity processing, IEEE (Inst. Electr. Electron. Eng.) Trans. Biomed. Eng. 63 (2015) 797–804.
[33] J.D. Hoffman, S. Frankel, Numerical Methods for Engineers and Scientists, second ed., CRC Press, 2001.
[34] Y. Kong, H.F. Posada-Quintero, K.H. Chon, Pain detection using a smartphone in real time, in: 2020 42nd Annual International Conference of the IEEE Engineering in Medicine & Biology Society (EMBC), IEEE, 2020, pp. 4526–4529.
[35] K.H. Chon, C.G. Scully, S. Lu, Approximate entropy for all signals, IEEE Eng. Med. Biol. Mag. 28 (2009) 18–23.
[36] S.M. Pincus, Approximate entropy as a measure of system complexity, Proc. Natl. Acad. Sci. USA 88 (1991) 2297–2301.
[37] Y. Kong, H.F. Posada-Quintero, K.H. Chon, Female–male differences should be considered in physical pain quantification based on electrodermal activity: preliminary study, in: 2021 43rd Annual International Conference of the IEEE Engineering in Medicine & Biology Society (EMBC), IEEE, 2021, pp. 6941–6944.
[38] N.V. Chawla, K.W. Bowyer, L.O. Hall, W.P. Kegelmeyer, SMOTE: synthetic minority over-sampling technique, J. Artif. Intell. Res. 16 (2002) 321–357.
[39] F. Seifert, N. Schuberth, R. De Col, E. Peltz, F.T. Nickel, C. Maihöfner, Brain activity during sympathetic response in anticipation and experience of pain, Hum. Brain Mapp. 34 (2013) 1768–1782.
[40] M. Kano, A.D. Farmer, Q. Aziz, V.P. Giampietro, M.J. Brammer, S.C.R. Williams, S. Fukudo, S.J. Coen, Sex differences in brain response to anticipated and experienced visceral pain in healthy subjects, Am. J. Physiol. Gastrointest. Liver Physiol. 304 (2013) G687, https://doi.org/10.1152/ajpgi.00385.2012. –G699.
[41] D.S. Bari, Gender differences in tonic and phasic electrodermal activity components, Sci. J. Univ. Zakho. 8 (2020) 29–33.
[42] M. Garwood, B.T. Engel, J.P. Kusterer, Skin potential level: age and epidermal hydration effects, J. Gerontol. 36 (1981) 7–13.
[43] C.S. Leithead, M.A. Pallister, Observations on dehydration and sweating, Lancet (1960) 114–117.